European Polymer Journal 62 (2015) 43–50

Contents lists available at ScienceDirect

European Polymer Journal

journal homepage: www.elsevier.com/locate/europolj

Molecular characterization of biodegradable natural resin acid-substituted polycaprolactone

Liang Yuan [b], Nasrollah Hamidi [a,*], Shaleesh Smith [a], Felicia Clemons [a], Amid Hamidi [a], Chuanbing Tang [b,*]

[a] Department of Biological and Physical Sciences, South Carolina State University, Orangeburg, South Carolina 29115, United States
[b] Department of Chemistry and Biochemistry, University of South Carolina, Columbia, South Carolina 29208, United States

ARTICLE INFO

Article history:
Received 4 October 2014
Received in revised form 29 October 2014
Accepted 30 October 2014
Available online 11 November 2014

Keywords:
Renewable polymer
Natural resources
Conformation
Rosin

ABSTRACT

Renewable resin acid-substituted polycaprolactone is prepared for characterization of physical properties of polymers. Six samples of dehydroabietic acid-substituted polycaprolactone (PCL-g-DAPE) with various molecular weight were synthesized by a combination of ring-opening polymerization and click chemistry. These polymers were characterized by on-line two angle light scattering and differential pressure viscosity. The values of *dn*/*dc*, average molecular weight, intrinsic viscosity, hydrodynamic radius, and radius of gyration were determined. Mark-Houwink double logarithmic relations of intrinsic viscosity and weight average molecular weight as well as Stockmayer–Fixman plots were established to scale the dimensions and conformation of PCL-g-DAPE chains related to their molar mass. The results indicated that PCL-g-DAPE is a flexible-coil polymer, similar to poly(methyl acrylate). Such properties were somewhat unexpected, considering the bulky group in the polymer side chains.

1. Introduction

Biodegradable polymers have gained much attention due to their potential applications in biomedical areas and utility as environment-friendly disposable packaging materials [1,2]. One important source of these polymers comes directly from natural biomass or can be synthesized by microorganisms [3]. Another scope of biodegradable polymers is classified as petroleum-derived synthetic polymers such as polycaprolactone [4]. By combining degradability of synthetic polymers and sustainability of renewable resources, biodegradable polymers based on natural resources have been developed, with new emerging properties originating from renewable resources [5].

Rosin is a renewable natural resource from the exudation of pine and conifer trees or from waste pulp in paper industry [6]. Its major components are resin acids, which have a bulky hydrophenanthrene group that can render hydrophobicity to any substrates it attaches. We have recently developed a platform of sustainable polymers and composites based on renewable rosin [7,8]. These materials include (meth)acrylic polymers by controlled polymerization [9], semi-degradable [10] or degradable polyesters by ring-opening polymerization [11], and lignin, cellulose composite polymers by surface-initiated polymerization [12,13].

These materials exhibit interesting properties including enhanced hydrophobicity, good thermal stability, fluorescent property and antimicrobial activities [12,14–16]. All polymers with rosin at the side chain are amorphous. However, most polymers are brittle, most likely due to the presence of the bulky hydrophenanthrene, which could result in

* Corresponding authors.
E-mail addresses: nhamidi@scsu.edu (N. Hamidi), tang4@mailbox.sc.edu (C. Tang).

http://dx.doi.org/10.1016/j.eurpolymj.2014.10.023
0014-3057/

a high entanglement molecular weight of polymers. One of intuitive questions is whether these polymers adopt a rigid conformation due to the bulky group or still exhibit a random-coil conformation. An in-depth understanding of their conformation would facilitate macromolecular design toward favorable mechanical properties. The influence of side chain groups on the physical properties of polyethylene chains is well documented [17]. In the case of polyacrylates, interests have been focused on the changes induced by altering the length of alkyl ester group [18] or identity of the ester linkage such as phenyl with alkyl substituent in various positions [19]. The methods of evaluating configurational properties are usually sought after two parameters theories, such as Mark-Houwink-Kuhn-Sakurada (MH) and Stockmayer–Fixman (SF) [20,21] relationships to viscosity and molar weight to estimate conformational properties including Flory's characteristic ratio (C_∞) [22–24].

Herein we present a case of model study to investigate some physical properties of a rosin-containing polyester by intrinsic viscosity and molar mass relationship based on MH and SF methods. We hope this study could shed light on many other types of polymers containing rosin moiety. This polyester is based on rosin-substituted polycaprolactone. Specifically, we prepared six samples of dehydroabietic acid-substituted polycaprolactone (PCL-g-DAPE) with different molecular weight via a click reaction between propargyl ester of dehydroabietic acid (DAPE) and an azide-substituted PCL.

All samples were characterized via a combination of online measurement of intrinsic viscosity, refractive index, and two-angle light scattering in a size exclusion chromatography [25]. The advantage of this method is that a single measurement could simultaneously yield characteristic parameters of macromolecules including weight-average molecular weight (M_w), number-average molecular weight (M_n), polydispersity (M_w/M_n), intrinsic viscosity [η], radius of gyration (R_g), hydrodynamics radius (R_h), and dn/dc of samples in solution.

2. Experimental

2.1. Materials

Standard calibration samples of polystyrene with narrow molecular mass distribution were purchased from Sigma–Aldrich; tetrahydrofuran (THF) was purchased from Fisher Scientific. Other solvents and reagents were purchased from the above mentioned companies and used without further treatment.

2.2. Synthesis of PCL-g-DAPE polymers

PCL-g-DAPE samples with different molecular weight were prepared according to our previous report [11]. The synthetic route is shown in Scheme 1. Propargyl ester of dehydroabietic acid (DAPE) and α-azide substituted poly(caprolactone) (P($\alpha N_3\varepsilon$CL)) with different molecular weight were first prepared. Through a copper-catalyzed (with CuI/DBU (1,8-diazabicyclo[5.4.0]undec-7-ene)) cycloaddition reaction between the azide group and the alkyne group, DAPE was grafted onto P($\alpha N_3\varepsilon$CL), resulting PCL-g-DAPE as our sample. The product was first purified by passing through a basic aluminum oxide column. The concentrated solution was then precipitated into a solution of ethylenediaminetetraacetic acid tetrasodium salt (EDTA) in a mixture of H_2O/CH_3OH, and washed with methanol before drying under vacuum. ^{1}H NMR spectra (Fig. 1) confirmed the successful preparation of the polymers. Using P($\alpha N_3\varepsilon$CL) with different molecular weight, six samples of PCL-g-DAPE with various molecular weight were prepared and named as samples A–F, in the trend of decreasing molecular weight.

2.3. Characterization

^{1}H NMR (300 MHz) spectra were recorded on a Varian Mercury spectrometer with tetramethylsilane (TMS) as an internal reference. The dilute solution viscosities were measured by Viscotek (Houston, TX) GPC-MAX 303 using various volume of the solution (15, 25, 35, 75, 95, 110, 130, 150 μL) of a given sample of PCL-g-DAPE in THF prepared a day before use. The solutions were prepared gravimetrically by measuring mass of solvent and solute using a Mettler-Toledo XS205 Dual-Range analytical balance with an uncertainty of 0.02 mg.

The Viscotek (USA) TDA consists of a 18 μL cell with a laser light at 760 nm, two-light scattering detectors, one at right angle and the other at low angle (~7°), a refractive index deflection type detector with reference cell volume 12 μL and light emitting diode (LED) at 660 nm wavelength, and a four capillary, differential Wheatstone bridge configuration viscometer with bridge volume about 72 μL.

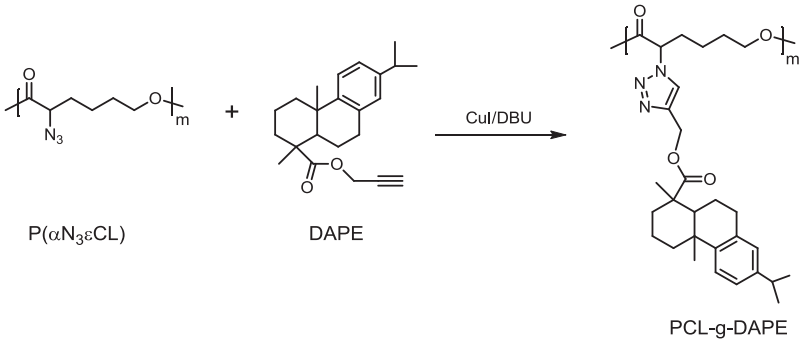

Scheme 1. Synthesis of PCL-g-DAPE polymers.

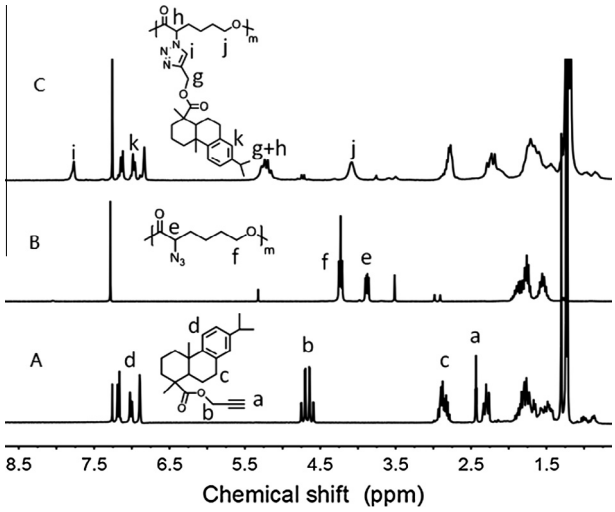

Fig. 1. ^{1}H NMR spectra of (A) DAPE, (B) P(αN$_3$CL), (C) PCL-g-DAPE.

The viscometry shear rate at a flow rate 3.0 mL/min in THF is ~3000 s^{-1}. The flow rate of PCL-g-DAPE in THF samples was 0.5 mL/min that results in a lower shear rate.

The Viscotek GPC-MAX autosampler uses a fixed 200 μL volume sample loop with variable injection volume syringes. It was programmed for two washes after each injection, and purging RI and DP cells five minutes before each injection. The standard 2 mL clear glass, screw cap vials were filled with 1.8 mL of a sample, then located in the corresponding vial rack number. Both detector and autosampler are controlled by a Dell PC running Omnisec 4.2 software. The GPC is equipped with two Viscogel-I series mixed bed columns (7.8 mm × 30 cm), I-MBLMW-3078 for low molar mass polymers (>20,000 g/mol) and I-MBHMW-3078 for higher molar mass polymers (>10,000,000 g/mol). The columns and all detectors are housed in the same thermostat oven at 50 °C. Differential scanning calorimetry (DSC) experiments were conducted on a DSC Q200 (TA Instruments). The samples were heated from 25 to 200 °C and then cooled to −70 °C at a rate of 10 °C/min. The data were collected from the second heating cycle (−70 to 200 °C). The sample weight was ~8 mg for each test, and the nitrogen flow rate was 40 mL/min.

3. Results and discussion

3.1. Refractive index increment

One of the physical properties of a polymer solution is refractive index increment (*dn*/*dc*). The accuracy of molecular weight determination by light scattering depends on the accuracy of *dn*/*dc*. This parameter indicates the change of refractive index versus concentration of a solution at a given temperature and a given wavelength of light. Typically higher increment values of refractive index indicate improved signal/noise ratio of light scattering detector and therefore more accurate molecular mass determination. Accurate *dn*/*dc* values can be obtained by plotting the refractive index of a polymer solution versus solution concentration or various volume of the same solution injected to SEC-TAD. The values of *dn*/*dc* obtained for each sample of PCL-g-DAPE are tabulated in Table 1.

Table 1
Molecular characterizations of PCL-g-DAPE in THF at 50 °C.

Parameter	Sample					
	A	B	C	D	E	F
M_n (kDa)	82.84	53.80	28.23	25.90	16.88	16.30
M_w (kDa)	100.53	59.50	36.59	31.47	21.20	17.50
M_w/M_n	1.21	1.10	1.30	1.21	1.26	1.08
[η] (mL/g)	13.29	10.70	8.49	7.24	5.86	4.74
R_h (nm)	4.14	3.83	3.56	3.57	3.22	2.42
R_g (nm)	46.65	38.62	N/A	N/A	N/A	N/A
dn/*dc* (ml/g)	0.0435	0.0737	0.0880	0.1126	0.0997	0.0987

Typically the values of *dn*/*dc* for most homo-polymers are nearly constant in a wide range of molar mass at a given temperature and solvent, like polystyrene in THF. However, our PCL-g-DAPE polymers in THF at 50 °C exhibit molecular weight dependent behavior of *dn*/*dc*, as shown in Fig. 2. Hence, it was appropriate to evaluate each sample

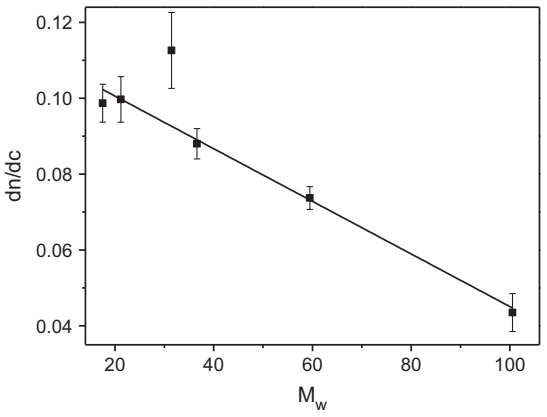

Fig. 2. A function of *dn*/*dc* versus M_w for PCL-g-DAPE samples in THF at 50 °C.

by its own *dn*/*dc* value, rather than taken an average value of *dn*/*dc* for all PCL-g-DAPE samples with different molecular weight.

3.2. Molecular weight characterization of PCL-g-DAPE

The molar mass of polymer samples was characterized by an on-line two-angle light scattering using the chromatograms utilizing the *dn*/*dc* value of each sample. In Fig. 3, the chromatograms showed the variation of PCL-g-DAPE concentrations versus retention volume as detected by four different detectors: DP, RALS, LALS, and RI. All are symmetric and clean of sparks. The dispersity of all samples was lower than 1.30. The precursor polymers P(αClεCL) were prepared by ROP, which is a controlled polymerization method and thus can make polymers with low dispersity. The molecular weight information is summarized in Table 1.

3.3. Intrinsic viscosity and molecular weight

The intrinsic viscosity $[\eta]$ of a polymer in a dilute solution is a measure of its hydrodynamic size and conformation [26]. The widely used relationship between $[\eta]$ and $\overline{M}_W$ is the Mark-Houwink-Kuhn-Sakurada (MH) relationship [27–29]:

$$[\eta] = K_v \overline{M}_w^v \quad (1)$$

where the parameter v is a measure of the thermodynamic power of the solvent and K_v is a measure of the coil volume under unperturbed conditions.

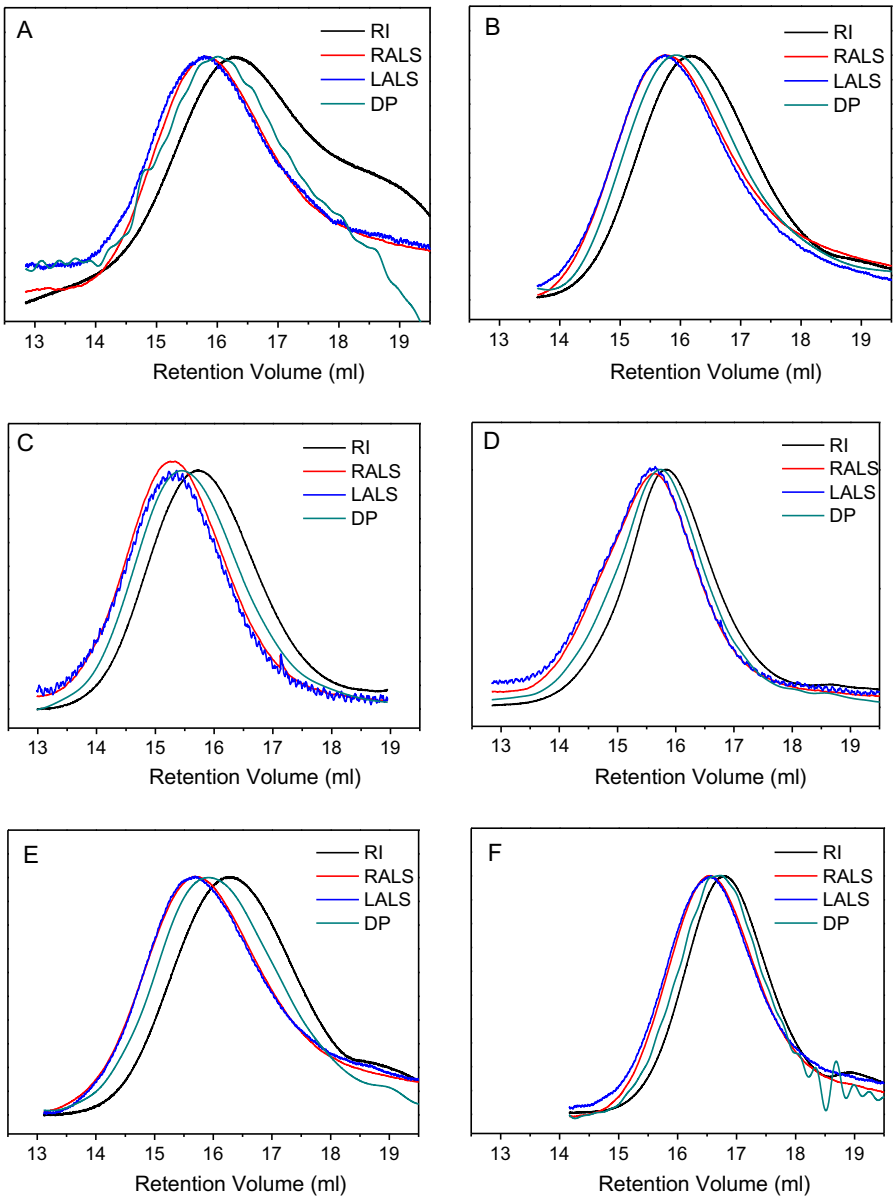

Fig. 3. DP, RALS, LALS, and RI chromatograms of PCL-g-DAPE (samples A–F).

Double logarithmic plot of MH for the dilute solution viscosity is a common method to obtain the dimensions of a polymer. A least-square line was fitted well into the PCL-g-DAPE experimental data with $v = 0.543$ and $K_v = 0.0268$ (cgs units) (Fig. 4). The v value for PCL-g-DAPE polymers is close to that for poly(methyl acrylate) (PMA) and poly(3,5-dimethylphenyl acrylate) (PDMPA) in toluene, indicating they behave as a non-ideal solution. Significantly, the PCL-g-DAPE solution behavior is different from the parent backbone polymer PCL, as shown in Table 2.

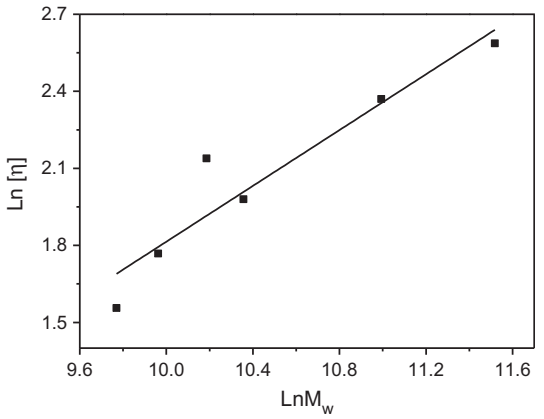

Fig. 4. The double logarithmic plot of intrisic viscosity versus M_w of PCL-g-DAPE.

Table 2
Solution properties of PCL-g-DAPE. The same parameters of polycaprolactone (PCL), atactic polypropylene (aPP), poly(methy acrylate) (PMA), poly(*iso*propyl fumarate) (PPF), and poly(3,5-dimethylphenyl acrylate) (PDMPA) are included for comparison.

Polymer	v	$K_v \times 10^3$	Solvent	T (°C)
PCL-g-DAPE	0.543	26.8	THF	50
PCL [30]	0.700	29	THF	25
aPP [27]	0.71	27	Benzene	25
PMA [21]	0.553	56.4	Toluene	30
PPF [31]	0.981	0.52	THF	30
PDMPA [32]	0.555	48.7	Toluene	40

3.4. Dependence of R_h on molecular weight of PCL-g-DAPE

For flexible polymers, the radius of gyration $\langle R_g^2\rangle^{1/2}$ is proportional to $M_w{}^{1/2}$ at a θ condition. In a good solvent, the polymer coil volume expands, thus the relationship changes to $\langle R_g{}^2\rangle^{1/2} \sim \alpha M_w{}^{1/2}$, with α being the expansion factor that is molecular weight dependent. Overall the general relationship is described by the following equation:

$$\langle R_g^2\rangle^{1/2} = k_\gamma M_w^\gamma \tag{2}$$

In a good solvent, both k_γ and γ are a function of the solvent quality and chain dimension [33]. Fig. 5 shows the double logarithmic variation of average of R_g and R_h versus M_w of the samples. The R_h data is well-described by the following power law:

$$R_h = 0.2422 M_w^{0.251} \tag{3}$$

For monodispersed rigid spheres, R_h and R_g radii are identical. For sufficiently long flexible polymer chains in good solvents, these radii are expected to differ from one another but to vary with molecular weight in the same way. Le Guillou and Zinn-Justin [34] predicted the proportionality of the $R_g \sim M_w{}^{0.588}$ for polystyrene under the asymptotic range of strong excluded volume effects. For PCL-g-DAPE that is a random flexible polymer, the R_h exponent was 0.251, which is lower than the predicted value for PS due to chemical differences in structure and influences of solvent. Unfortunately, we could only obtain two reliable R_g values, probably due to the limited range of molecular weight of these polymers.

3.5. Evaluation of conformational characteristics

Flory characteristic ratio C_∞ and steric factor σ are two factors used to evaluate the rigidity of a polymer in solution. The C_∞ relates to the freely jointed model, in which only bond lengths are fixed, whereas the mutual orientations of skeletal bonds are random. Therefore, the C_∞ is the random-coil limit of the ratio of the unperturbed mean-square end-to-end distance of the real chain ($\langle R^2\rangle_0$) to a hypothetical free random flight chain ($\langle R^2\rangle_{00}$). This reflects restrictions on all directional correlations of skeletal bonds in the real chain.

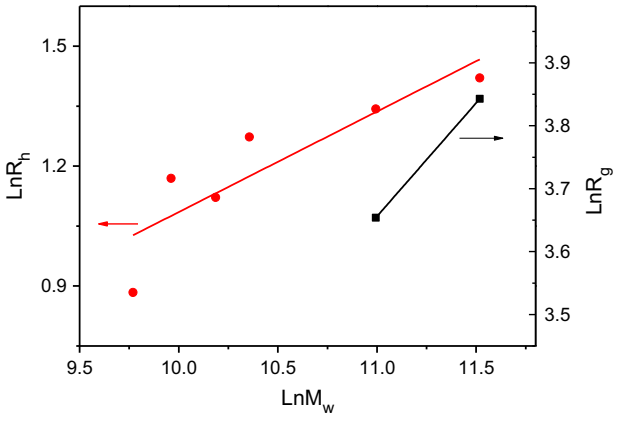

Fig. 5. Radius of gyration (R_g) and hydrodynamic radius (R_h) as a function of molecular weight for PCL-g-DAPE.

$$C_\infty = \frac{\lim_{n\to\infty}\left\langle R^2\right\rangle_0}{\sum_i n_i l_i} = \left(\frac{\left\langle R^2\right\rangle_0}{\left\langle R^2\right\rangle_{00}}\right)^{1/2} \quad (4)$$

The σ reflects the effect of hindrance to free rotation of a bond around the main chain bonds, defined as:

$$\sigma = \left(\frac{\langle R^2\rangle_0}{\langle R^2\rangle_{0f}}\right)^{1/2} \quad (5)$$

where $\langle R^2\rangle_{0f}$ reflects the freely rotating state of a hypothetical state of a polymer chain in which the bond angle restrictions are retained, but the steric hindrance to internal rotation is allowed. The mean-square end-to-end distance of the freely rotating chain that consists of only one kind of bond of length l is: [35]

$$\langle R^2\rangle_{0f} = nl^2\frac{(1-\cos\theta)}{(1+\cos\theta)} \quad (6)$$

For polymer chains in an ideal solution, the value of $\langle R^2\rangle_0$ may be obtained directly from the intercept of the MHKS plot. For non-ideal solutions, such as the case of PCL-g-DAPE in THF at 50 °C, the unperturbed dimensions are characterized by extrapolation methods using a number of plots based on theoretical or semi-theoretical equations developed for this purpose, i.e., applications of the excluded volume equations to the molecular weight and intrinsic viscosity of homologues series of polymers in a good solvent. Stockmayer–Fixman [20] proposed one such relationship for treating data covering the usual range of molecular weights encountered in experiments:

$$[\eta]M_w^{-\frac{1}{2}} = K_\theta + 0.346\Phi_0 BM_w^{\frac{1}{2}} \quad 0 \le \alpha^3 \le 1.6 \quad (7)$$

Φ is Flory's universal viscosity constant. For infinite molar mass when $[\eta]$ expressed in mL/g, the theoretical value of Φ_∞ is 2.87×10^{23} mol^{-1} (cgs) [23]. For narrow molecular weight distribution, the value of $\Phi_0 = 2.7\times10^{23}$ is used [27]. The expansion factor, α, of PCL-g-DAPE in THF was estimated by:

$$\alpha = [\eta]/K_\theta M_w^{1/2} \quad (8)$$

where K_θ was estimated from the intercept of SF relationship. The values of α were below 1.6 for all samples, therefore, Eq. (7) was applicable to the data. The plot of $[\eta]M^{-1/2}$ against $\langle M_w\rangle^{1/2}$ is shown in Fig. 6. The value of K_θ is estimated by fitting a least-square straight line into data points (except the very lower M_W). Table 3 shows the molecular parameters of PCL-g-DAPE.

The constant K_θ of S–F relationship is related to the unperturbed dimension of the polymer:

$$K_\theta = \Phi_0\left(\frac{\langle R^2\rangle_0}{M_w}\right)^{3/2} \quad (9)$$

The dimensional parameters of poly(methyl methacrylate) (PMA), polypropylene (PP) polycaprolactone (PCL), poly(diisopropyl fumarate) (PPF), and poly(3,5-dimethylphenyl acrylate) (PDPMA) are included for comparison. The obtained $K_\theta = 0.035$ cm^3 g$^{-3/2}$ mol^{½} is lower than of PMA, PDPMA and PCL. Therefore, the unperturbed

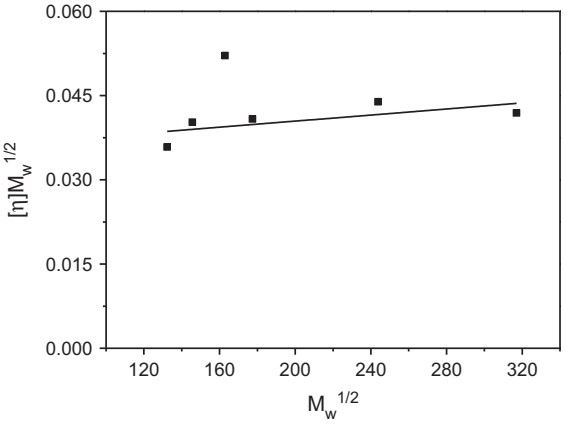

Fig. 6. Stockmayer–Fixman plot for PCL-g-DAPE samples in THF at 50 °C.

Table 3
Dimensional parameters for PCL-g-DAPE and others polymers, including K_θ, $(\langle R^2\rangle_0/M_w)^{1/2}$, σ, C_∞ and B.

Polymer	K_θ (cgs)	$(\langle R^2\rangle_0/M_w)^{1/2}$ (Å)	σ	C_∞	$B\times10^{29}$
PCL-g-DAPE	0.035	0.571	2.18	9.5	10.6
PCL	0.12	0.783	1.45	4.9	380[a]
a-PP	0.165	0.835	1.76	6.2	N/A
PMA	0.0948	0.706	2.13	9.0	28.9
PPF	0.0341	0.502	3.26	10.6	191[a]
PDMPA	0.1040	0.728	3.14	19.7	1.91

[a] Calculated using reported intrinsic viscosity and molecular weight.

dimension of PCL-g-DAPE was smaller than other mentioned polymers in THF, indicating that THF is a good thermodynamic solvent for other polymers, and a thermodynamically weak solvent for PCL-g-DAPE.

Another argument to justify the lower value of end-to-end dimensions of PCL-g-DAPE in THF at 50 °C is concealed for the method of evaluation. Based on Eq. (7) the plot of $[\eta]$ $M_w{}^{1/2}$ versus $M_w{}^{1/2}$ should be linear only for long enough chains ($n > 10^3$), where the excluded volume parameter approaches its limit. A visual inspection of Fig. 6 shows the lower-molecular-weight sample does not meet these conditions. The data in general are scattered; however, the plateau of the data at higher M_w is visible. Thus, precaution is necessary to evaluate dimensional parameters based on the SF relationship under this condition. For an ideal solvent, the slope of the SF equation should be zero. The slope observed for PCL-g-DAPE in THF at 50 °C is not zero (2.7×10^{-5}). This corroborated with the value of MH exponent ($v = 0.543$), which indicated the PCL-g-DAPE-THF system at 50 °C is near to an ideal solution.

In the freely rotating model, rotation about the main chain bonds is free. In this case, the conformation of PCL-g-DAPE chains in THF can be characterized by the σ (Eq. (5)). The $\langle R^2\rangle_0$ is obtained experimentally from of SF relationship (Eq (9)). The value of $\sigma = 2.18$ for PCL-g-DAPE-THF is tabulated in Table 3 along with PCL, other acrylic and methacrylic polymers for comparison. The higher σ value for PCL-g-DAPE-THF reflects the effect of hindrance to free rotation, which falls in range of the σ

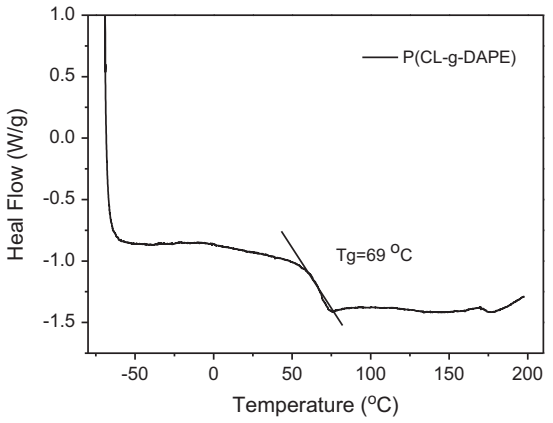

Fig. 7. DSC trace of PCL-g-DAPE polymer (sample F from Table 1).

values found for most of the acrylic flexible polymers ($1.5 < \sigma < 2.5$). For example, the σ value for PMA in toluene is 2.08. For more rigid acrylic polymers (PDMPA), the σ value is around 3 due to the effects of the orientation of the lateral groups. The σ value for PCL-g-DAPE in THF was larger than the σ value of PCL (1.45). This is due to the effects of bulky lateral groups (DAPE) that induce restrictions to the free rotation of main chain.

The value of C_∞ based on Eq. (4) for PCL-g-DAPE is also tabulated in Table 3. The value of $C_\infty = 9.5$ for PCL-g-DAPE in THF at 50 °C falls within the C_∞ values for atactic vinyl polymers with aliphatic side chains, which are in the range of $5 < C_\infty < 10$. The value of C_∞ of acrylic rigid polymers, such as PDMPA in EA was found to be about 18.5–18.9; therefore, the value of C_∞ of PCL-g-DAPE falls within flexible polymers. The C_∞ of PCL-g-DAPE in THF at 50 °C (9.5) is larger than the C_∞ of PCL (4.9). This reflects the restriction induced by DAPE groups to the main chain of PCL and corroborates well with the σ values of both polymers.

One possible reason of the coil conformation of PCL-g-DAPE may be due to the contribution from the flexible spacer between the backbone and bulky substituted group. In addition, differential scanning calorimetry analysis (Fig. 7) showed that regardless of molecular weight, all samples just exhibited glass transitions without the presence of melting, thus ruling out the possibility of crystalline (or liquid crystalline) properties from these polymers.

4. Conclusions

A series of resin acid-grafted PCL polymers (PCL-g-DAPE) with different molecular weight were prepared by a combination of ROP and click chemistry. The samples were characterized by on-line two angle light scattering and differential pressure viscosity to determine the characteristic parameters of the polymer. The refractive index increment dn/dc for PCL-g-DAPE samples was found to be dependent upon the molecular weight of samples. The PCL-g-DAPE system in THF at 50 °C was described well with MH relationship, which indicates that PCL-g-DAPE behaves similarly to the non-ideal solution of PMA in toluene.

The steric factor σ (=2.18) of PCL-g-DAPE in THF at 50 °C falls within the values of random flexible polymer chains such as PMA. However, the σ Value of PCL-g-DAPE was larger than PCL due to restrictions to the polymer main chain induced by bulky DAPE side chains groups. The Flory characteristic ratio C_∞ (=9.5) of PCL-g-DAPE was also in the range of the values for random coil macromolecules like PMA. However, it is higher than more flexible polymers, such as PCL, because the grafted DAPE side groups induce restrictions to the free rotation of the main chain.

Acknowledgements

This project is based upon work supported by the National Science Foundation/EPSCoR under Grant No. OIA 1317771 and the subcontract 13-105 to South Carolina State University.

References

[1] Gross RA, Kalra B. Biodegradable polymers for the environment. Science 2002;297:803–7.
[2] Amass W, Amass A, Tighe B. A review of biodegradable polymers: uses, current developments in the synthesis and characterization of biodegradable polyesters, blends of biodegradable polymers and recent advances in biodegradation studies. Polym Int 1998;47:89–144.
[3] Ravi Kumar MN. A review of chitin and chitosan applications. React Funct Polym 2000;46:1–27.
[4] Woodruff MA, Hutmacher DW. The return of a forgotten polymer – polycaprolactone in the 21st century. Prog Polym Sci 2010;35:1217–56.
[5] Okada M, Okada Y, Tao A, Aoi K. Biodegradable polymers based on renewable resources: polyesters composed of 1, 4:3, 6-dianhydrohexitol and aliphatic dicarboxylic acid units. J Appl Polym Sci 1996;62:2257–65.
[6] Maiti S, Ray SS, Kundu AK. Rosin: a renewable resource for polymers and polymer chemicals. Prog Polym Sci 1989;14:297–338.
[7] Yao K, Tang C. Controlled polymerization of next-generation renewable monomers and beyond. Macromolecules 2013;46:1689–712.
[8] Wilbon PA, Chu F, Tang C. Progress in renewable polymers from natural terpenes, terpenoids, and rosin. Macromol Rapid Commun 2013;34:8–37.
[9] Zheng Y, Yao K, Lee J, Chandler D, Wang J, Wang C, et al. Well-defined renewable polymers derived from gum rosin. Macromolecules 2010;43:5922–4.
[10] Wilbon PA, Zheng Y, Yao K, Tang C. Renewable rosin acid-degradable caprolactone block copolymers by atom transfer radical polymerization and ring-opening polymerization. Macromolecules 2010;43:8747–54.
[11] Yao K, Wang J, Zhang W, Lee JS, Wang C, Chu F, et al. Degradable rosin-ester-caprolactone graft copolymers. Biomacromolecules 2011;12:2171–7.
[12] Wang J, Yao K, Korich AL, Li S, Ma S, Ploehn HJ, et al. Combining renewable gum rosin and lignin: towards hydrophobic polymer composites by controlled polymerization. J Polym Sci, Part A: Polym Chem 2011;49:3728–38.
[13] Liu Y, Yao K, Chen X, Wang J, Wang Z, Ploehn HJ, et al. Sustainable thermoplastic elastomers derived from renewable cellulose, rosin and fatty acids. Polym Chem 2014;5:3170–81.
[14] Wang J, Chen YP, Yao K, Wilbon PA, Zhang W, Ren L, et al. Robust antimicrobial compounds and polymers derived from natural resin acids. Chem Commun 2012;48:916–8.
[15] Chen Y, Wilbon PA, Zhou J, Nagarkatti M, Wang C, Chu F, et al. Multifunctional self-fluorescent polymer nanogels for label-free imaging and drug delivery. Chem Commun 2013;49:297–9.
[16] Wang J, Yao K, Wang C, Tang C, Jiang X. Synthesis and drug delivery of novel amphiphilic block copolymers containing hydrophobic dehydroabietic moiety. J Mater Chem B 2013;1:2324–32.

[17] Flory P, Volkenstein M. Statistical mechanics of chain molecules. Wiley Online Library; 1969.
[18] Xu Z, Hadjichristidis N, Fetters LJ. Solution properties and chain dimensions of poly(n-alkyl methacrylates). Macromolecules 1984;17:2303–6.
[19] Gargallo L, Hamidi N, Radic D. Synthesis, solution properties and chain flexibility of poly (2,6-dimethylphenyl methacrylate). Polymer 1990;31:924–7.
[20] Stockmayer W, Fixman M. On the estimation of unperturbed dimensions from intrinsic viscositiesxcin. J Polym Sci C: Polym Symp 1963;1:137–41.
[21] Ikeda H, Shima H. Solution properties of polymethyl acrylate I. Properties of PMA chain by viscometric method. Eur Polymer J 2004;40:1565–74.
[22] Abe Y, Flory PJ. Configurational statistics of 1,4-polybutadiene chains. Macromolecules 1971;4:219–29.
[23] Yamakawa H, Fujii M. Intrinsic viscosity of wormlike chains. determination of the shift factor. Macromolecules 1974;7:128–35.
[24] Bohdanecky M. New method for estimating the parameters of the wormlike chain model from the intrinsic viscosity of stiff-chain polymers. Macromolecules 1983;16:1483–92.
[25] Terao K, Mays JW. On-line measurement of molecular weight and radius of gyration of polystyrene in a good solvent and in a theta solvent measured with a two-angle light scattering detector. Eur Polymer J 2004;40:1623–7.
[26] Yoon D, Sundararajan P, Flory P. Conformational characteristics of polystyrene. Macromolecules 1975;8:776–83.
[27] Brandrup J, Immergut EH, Grulke EA, Abe A, Bloch DR. Polymer handbook, vol. 89. New York: Wiley; 1999.
[28] Yamakawa H. Modern theory of polymer solutions. New York: Harper & Row; 1971.
[29] Morawetz H. Macromolecules in solution, vol. 21. New York: Springer; 1965.
[30] Huang Y, Xu Z, Huang Y, Ma D, Yang J, Mays JW. Characterization of poly (ε-caprolactone) via size exclusion chromatography with online right-angle laser-light scattering and viscometric detectors. Int J Polym Anal Charact 2003;8:383–94.
[31] Matsumoto A, Nakagawa E. Evaluation of chain rigidity of poly (diisopropyl fumarate) from light scattering and viscosity in tetrahydrofuran. Eur Polymer J 1999;35:2107–13.
[32] Hamidi N. Synthesis and characterization of poly (3,5-dimethylphenylacrylate) in toluene at 40 °C by two-angle light-scattering and differential pressure viscometry. Inter J Appl 2012;2:7–23.
[33] Hong F, Lu Y, Li J, Shi W, Zhang G, Wu C. Revisiting of dimensional scaling of linear chains in dilute solutions. Polymer 2010;51:1413–7.
[34] Le Guillou J, Zinn-Justin J. Critical exponents for the *n*-vector model in three dimensions from field theory. Phys Rev Lett 1977;39:95–8.
[35] Tonelli AE. NMR spectroscopy and polymer microstructure: the conformational connection. New York: VCH; 1989.